EUROPEAN ORGANIZATION FOR NUCLEAR RESEARCH

CERN-PPE/95-020
February 27, 1995

An Improved Measurement of the B_s^0 Lifetime

The OPAL Collaboration

Abstract

This letter presents an updated measurement of the lifetime of the B_s^0 meson using 3.6 million hadronic Z^0 decays recorded by the OPAL detector at LEP from 1990 to 1994. A sample of B_s^0 decays is obtained using $D_s^- \ell^+$ combinations, where the D_s^- is reconstructed in either the $\phi\pi^-$ or $K^{*0}K^-$ decay mode. From 79 ± 13 $D_s\ell$ combinations attributed to B_s^0 decays in this data sample, we measure

$$\tau(B_s^0) = 1.54^{+0.25}_{-0.21} \pm 0.06 \,\mathrm{ps},$$

where the errors are statistical and systematic, respectively.

(Submitted to Physics Letters B)

The OPAL Collaboration

R. Akers[16], G. Alexander[23], J. Allison[16], K. Ametewee[25], K.J. Anderson[9], S. Arcelli[2], S. Asai[24], D. Axen[29], G. Azuelos[18,a], A.H. Ball[17], E. Barberio[26], R.J. Barlow[16], R. Bartoldus[3], J.R. Batley[5], G. Beaudoin[18], A. Beck[23], G.A. Beck[13], C. Beeston[16], T. Behnke[27], K.W. Bell[20], G. Bella[23], S. Bentvelsen[8], P. Berlich[10], S. Bethke[32], O. Biebel[32], I.J. Bloodworth[1], P. Bock[11], H.M. Bosch[11], M. Boutemeur[18], S. Braibant[12], P. Bright-Thomas[25], R.M. Brown[20], A. Buijs[8], H.J. Burckhart[8], R. Bürgin[10], C. Burgard[27], N. Capdevielle[18], P. Capiluppi[2], R.K. Carnegie[6], A.A. Carter[13], J.R. Carter[5], C.Y. Chang[17], C. Charlesworth[6], D.G. Charlton[1,b], S.L. Chu[4], P.E.L. Clarke[15], J.C. Clayton[1], S.G. Clowes[16], I. Cohen[23], J.E. Conboy[15], O.C. Cooke[16], M. Cuffiani[2], S. Dado[22], C. Dallapiccola[17], G.M. Dallavalle[2], C. Darling[31], S. De Jong[12], L.A. del Pozo[8], H. Deng[17], M. Dittmar[4], M.S. Dixit[7], E. do Couto e Silva[12], J.E. Duboscq[8], E. Duchovni[26], G. Duckeck[8], I.P. Duerdoth[16], U.C. Dunwoody[5], J.E.G. Edwards[16], P.A. Elcombe[5], P.G. Estabrooks[6], E. Etzion[23], H.G. Evans[9], F. Fabbri[2], B. Fabbro[21], M. Fanti[2], P. Fath[11], M. Fierro[2], M. Fincke-Keeler[28], H.M. Fischer[3], P. Fischer[3], R. Folman[26], D.G. Fong[17], M. Foucher[17], H. Fukui[24], A. Fürtjes[8], P. Gagnon[6], A. Gaidot[21], J.W. Gary[4], J. Gascon[18], N.I. Geddes[20], C. Geich-Gimbel[3], S.W. Gensler[9], F.X. Gentit[21], T. Geralis[20], G. Giacomelli[2], P. Giacomelli[4], R. Giacomelli[2], V. Gibson[5], W.R. Gibson[13], J.D. Gillies[20], J. Goldberg[22], D.M. Gingrich[30,a], M.J. Goodrick[5], W. Gorn[4], C. Grandi[2], E. Gross[26], J. Hagemann[27], G.G. Hanson[12], M. Hansroul[8], C.K. Hargrove[7], P.A. Hart[9], M. Hauschild[8], C.M. Hawkes[8], E. Heflin[4], R.J. Hemingway[6], G. Herten[10], R.D. Heuer[8], J.C. Hill[5], S.J. Hillier[8], T. Hilse[10], P.R. Hobson[25], D. Hochman[26], R.J. Homer[1], A.K. Honma[28,a], R. Howard[29], R.E. Hughes-Jones[16], P. Igo-Kemenes[11], D.C. Imrie[25], A. Jawahery[17], P.W. Jeffreys[20], H. Jeremie[18], M. Jimack[1], M. Jones[6], R.W.L. Jones[8], P. Jovanovic[1], C. Jui[4], D. Karlen[6], J. Kanzaki[24], K. Kawagoe[24], T. Kawamoto[24], R.K. Keeler[28], R.G. Kellogg[17], B.W. Kennedy[20], B. King[8], J. King[13], J. Kirk[29], S. Kluth[5], T. Kobayashi[24], M. Kobel[10], D.S. Koetke[6], T.P. Kokott[3], S. Komamiya[24], R. Kowalewski[8], T. Kress[11], P. Krieger[6], J. von Krogh[11], P. Kyberd[13], G.D. Lafferty[16], H. Lafoux[8], R. Lahmann[17], W.P. Lai[19], J. Lauber[8], J.G. Layter[4], P. Leblanc[18], A.M. Lee[31], E. Lefebvre[18], D. Lellouch[26], C. Leroy[18], J. Letts[2], L. Levinson[26], S.L. Lloyd[13], F.K. Loebinger[16], G.D. Long[17], B. Lorazo[18], M.J. Losty[7], X.C. Lou[8], J. Ludwig[10], A. Luig[10], M. Mannelli[8], S. Marcellini[2], C. Markus[3], A.J. Martin[13], J.P. Martin[18], T. Mashimo[24], W. Matthews[25], P. Mättig[3], U. Maur[3], J. McKenna[29], T.J. McMahon[1], A.I. McNab[13], F. Meijers[8], F.S. Merritt[9], H. Mes[7], A. Michelini[8], R.P. Middleton[20], G. Mikenberg[26], D.J. Miller[15], R. Mir[26], W. Mohr[10], A. Montanari[2], T. Mori[24], M. Morii[24], U. Müller[3], B. Nellen[3], B. Nijjhar[16], S.W. O'Neale[1], F.G. Oakham[7], F. Odorici[2], H.O. Ogren[12], N.J. Oldershaw[16], C.J. Oram[28,a], M.J. Oreglia[9], S. Orito[24], F. Palmonari[2], J.P. Pansart[21], G.N. Patrick[20], M.J. Pearce[1], P.D. Phillips[16], J.E. Pilcher[9], J. Pinfold[30], D.E. Plane[8], P. Poffenberger[28], B. Poli[2], A. Posthaus[3], T.W. Pritchard[13], H. Przysiezniak[30], M.W. Redmond[8], D.L. Rees[8], D. Rigby[1], M.G. Rison[5], S.A. Robins[13], D. Robinson[5], N. Rodning[30], J.M. Roney[28], E. Ros[8], A.M. Rossi[2], M. Rosvick[28], P. Routenburg[30], Y. Rozen[8], K. Runge[10], O. Runolfsson[8], D.R. Rust[12], M. Sasaki[24], C. Sbarra[2], A.D. Schaile[8], O. Schaile[10], F. Scharf[3], P. Scharff-Hansen[8], P. Schenk[4], B. Schmitt[3], M. Schröder[8], H.C. Schultz-Coulon[10], P. Schütz[3], M. Schulz[8], C. Schwick[27], J. Schwiening[3], W.G. Scott[20], M. Settles[12], T.G. Shears[5], B.C. Shen[4], C.H. Shepherd-Themistocleous[7], P. Sherwood[15], G.P. Siroli[2], A. Skillman[15], A. Skuja[17], A.M. Smith[8], T.J. Smith[28], G.A. Snow[17], R. Sobie[28], S. Söldner-Rembold[10], R.W. Springer[30], M. Sproston[20], A. Stahl[3], M. Starks[12], C. Stegmann[10], K. Stephens[16], J. Steuerer[28], B. Stockhausen[3], D. Strom[19], P. Szymanski[20], R. Tafirout[18], H. Takeda[24], T. Takeshita[24], P. Taras[18], S. Tarem[26], M. Tecchio[9], P. Teixeira-Dias[11], N. Tesch[3], M.A. Thomson[8], O. Tousignant[18], S. Towers[6], M. Tscheulin[10], T. Tsukamoto[24], A.S. Turcot[9], M.F. Turner-Watson[8], P. Utzat[11], R. Van Kooten[12], G. Vasseur[21], P. Vikas[18], M. Vincter[28], A. Wagner[27], D.L. Wagner[9], C.P. Ward[5], D.R. Ward[5], J.J. Ward[15], P.M. Watkins[1], A.T. Watson[1],

N.K. Watson[7], P. Weber[6], P.S. Wells[8], N. Wermes[3], B. Wilkens[10], G.W. Wilson[27], J.A. Wilson[1], V-H. Winterer[10], T. Wlodek[26], G. Wolf[26], S. Wotton[11], T.R. Wyatt[16], A. Yeaman[13], G. Yekutieli[26], M. Yurko[18], V. Zacek[18], W. Zeuner[8], G.T. Zorn[17].

[1]School of Physics and Space Research, University of Birmingham, Birmingham B15 2TT, UK
[2]Dipartimento di Fisica dell' Università di Bologna and INFN, I-40126 Bologna, Italy
[3]Physikalisches Institut, Universität Bonn, D-53115 Bonn, Germany
[4]Department of Physics, University of California, Riverside CA 92521, USA
[5]Cavendish Laboratory, Cambridge CB3 0HE, UK
[6]Carleton University, Department of Physics, Colonel By Drive, Ottawa, Ontario K1S 5B6, Canada
[7]Centre for Research in Particle Physics, Carleton University, Ottawa, Ontario K1S 5B6, Canada
[8]CERN, European Organisation for Particle Physics, CH-1211 Geneva 23, Switzerland
[9]Enrico Fermi Institute and Department of Physics, University of Chicago, Chicago IL 60637, USA
[10]Fakultät für Physik, Albert Ludwigs Universität, D-79104 Freiburg, Germany
[11]Physikalisches Institut, Universität Heidelberg, D-69120 Heidelberg, Germany
[12]Indiana University, Department of Physics, Swain Hall West 117, Bloomington IN 47405, USA
[13]Queen Mary and Westfield College, University of London, London E1 4NS, UK
[15]University College London, London WC1E 6BT, UK
[16]Department of Physics, Schuster Laboratory, The University, Manchester M13 9PL, UK
[17]Department of Physics, University of Maryland, College Park, MD 20742, USA
[18]Laboratoire de Physique Nucléaire, Université de Montréal, Montréal, Quebec H3C 3J7, Canada
[19]University of Oregon, Department of Physics, Eugene OR 97403, USA
[20]Rutherford Appleton Laboratory, Chilton, Didcot, Oxfordshire OX11 0QX, UK
[21]CEA, DAPNIA/SPP, CE-Saclay, F-91191 Gif-sur-Yvette, France
[22]Department of Physics, Technion-Israel Institute of Technology, Haifa 32000, Israel
[23]Department of Physics and Astronomy, Tel Aviv University, Tel Aviv 69978, Israel
[24]International Centre for Elementary Particle Physics and Department of Physics, University of Tokyo, Tokyo 113, and Kobe University, Kobe 657, Japan
[25]Brunel University, Uxbridge, Middlesex UB8 3PH, UK
[26]Particle Physics Department, Weizmann Institute of Science, Rehovot 76100, Israel
[27]Universität Hamburg/DESY, II Institut für Experimental Physik, Notkestrasse 85, D-22607 Hamburg, Germany
[28]University of Victoria, Department of Physics, P O Box 3055, Victoria BC V8W 3P6, Canada
[29]University of British Columbia, Department of Physics, Vancouver BC V6T 1Z1, Canada
[30]University of Alberta, Department of Physics, Edmonton AB T6G 2J1, Canada
[31]Duke University, Dept of Physics, Durham, NC 27708-0305, USA
[32]Technische Hochschule Aachen, III Physikalisches Institut, Sommerfeldstrasse 26-28, D-52056 Aachen, Germany

[a]Also at TRIUMF, Vancouver, Canada V6T 2A3
[b] Royal Society University Research Fellow

1 Introduction

The lifetimes of b-flavored hadrons are related to both the strength of the b quark coupling to c and u quarks, and the dynamics of b hadron decay. The spectator model assumes that the light quarks in b and c hadrons do not affect the decay of the heavy quark, and thus predicts the lifetimes of all b hadrons to be equal. For charm hadrons this prediction is inaccurate; the measured D^+ lifetime is approximately 2.5 times that of the D^0 and more than twice that of the D_s [1]. More sophisticated models predict that the differences among b hadron lifetimes should be much smaller than those in the charm system, because of the larger mass of the b quark [2, 3]. These models predict a difference in lifetime between the B^+ and B^0 meson of several percent, and between the B_s^0 and B^0 meson of about 1% [3]. OPAL [4], and other collaborations [5], have published measurements of the B_s^0 lifetime.

In this letter, we present an updated measurement of the lifetime of the B_s^0 meson, which supersedes our previous measurement [4]. The two decay channels used are:[1]

$$\begin{array}{l} B_s^0 \to D_s^- \, \ell^+ \, \nu \, (X) \\ \qquad \hookrightarrow K^{*0} K^- \\ \qquad\quad \hookrightarrow K^+ \pi^- \end{array} \qquad \text{and} \qquad \begin{array}{l} B_s^0 \to D_s^- \, \ell^+ \, \nu \, (X) \\ \qquad \hookrightarrow \phi \, \pi^- \\ \qquad\quad \hookrightarrow K^+ K^- \; . \end{array}$$

where ℓ is an electron or a muon. The proper decay time is determined on an event-by-event basis using measured decay lengths and estimates of the B_s^0 energy. The following sections describe the OPAL detector, the selection of B_s^0 candidates, the vertex topology of the events, the determination of the B_s^0 decay length, the estimation of the B_s^0 energy, the lifetime fit, the results, and the systematic errors.

2 The OPAL Detector

The OPAL detector is described in reference [6]. The central tracking system is composed of a precision vertex drift chamber, a large volume jet chamber surrounded by a set of chambers to measure the z-coordinate (z-chambers) and, for the majority of the data used in this analysis, a high-precision silicon microvertex detector. These detectors are located inside a solenoidal coil.[2] The detectors outside the solenoid consist of a time-of-flight scintillator array and a lead glass electromagnetic calorimeter with a presampler, followed by a hadron calorimeter consisting of the instrumented return yoke of the magnet, and several layers of muon chambers. Charged particles are identified by their specific energy loss, $\mathrm{d}E/\mathrm{d}x$, in the jet chamber. Further information on the performance of the tracking and $\mathrm{d}E/\mathrm{d}x$ measurements can be found in reference [7].

[1] In this paper, charge conjugate modes are always implied. Also, unless otherwise noted, K and π always refer to charged particles.

[2] The coordinate system is defined such that the z-axis follows the electron beam direction and the x-y plane is perpendicular to it with the x-axis lying approximately horizontally. The polar angle θ is defined relative to the $+z$-axis, and the azimuthal angle ϕ is defined relative to the $+x$-axis.

3 B_s^0 Candidate Selection

This analysis uses data collected during the 1990–1994 LEP running periods at center-of-mass energies within $\pm 3\,\mathrm{GeV}/c^2$ of the Z^0 mass. After the standard hadronic event selection [8] and detector performance requirements, a sample of 3.6 million events is selected. Jets are defined using charged tracks and electromagnetic clusters not associated with a charged track. These are combined into jets using the scaled invariant mass algorithm with the E0 recombination scheme [9] using $y_{cut} = 0.04$. Tracks arising from identified secondary vertices due to decays of Λ, K_s^0 or γ conversions are excluded from the B_s^0 candidate selection.

3.1 $D_s^- \to K^+K^-\pi^-$ selection

In this analysis, D_s candidates are reconstructed in two modes. The first is $D_s^- \to K^{*0}K^-$ in which the K^{*0} decays into a $K^+\pi^-$. The second is $D_s^- \to \phi\pi^-$ where the ϕ subsequently decays into K^+K^-. When searching for D_s candidates, all combinations of tracks which are within a single jet and constitute the appropriate charge combination are considered.

Particle identification is used to reduce the combinatorial background. For each track forming the $KK\pi$ combination, the measured dE/dx is compared with the expected value, and the probability that it is consistent with a given mass assignment is required to be greater than 1%. If the observed energy loss of each kaon candidate is greater than the mean dE/dx expected for a kaon, it is required that the product of the two dE/dx probabilities be greater than .02. In order to improve the mass and decay length resolutions, at least two of the three candidate tracks are required to have good θ measurements either from the z-chambers or from a measurement of the track's endpoint as it exits the main jet chamber. The $KK\pi$ combination is required to have a momentum greater than $9\,\mathrm{GeV}/c$ in order to reduce random track combinations.

For the $K^{*0}K^-$ mode, the invariant mass of the $K\pi$ combination taken to be the K^{*0} is required to satisfy $0.845 < m_{K\pi} < 0.945\,\mathrm{GeV}/c^2$. To minimize the possibility of mistaking a $D^- \to K^{*0}\pi^-$ decay for our desired signal, the measured dE/dx of the kaon candidate directly from the D_s decay must be at least one standard deviation below the mean dE/dx that is expected for a pion. This track must also have a momentum greater than $2\,\mathrm{GeV}/c$ in order to be in the momentum region of good kaon-pion separation. If the observed energy loss of this track is greater than the mean expected for a kaon, it must have a dE/dx probability assuming a kaon hypothesis that is greater than 5%. In the $\phi\pi$ mode, the K^+K^- invariant mass is dominated by detector resolution and is required to satisfy $1.005 < m_{KK} < 1.035\,\mathrm{GeV}/c^2$.

The differences between the angular distributions of D_s decays and those of random track combinations are used to suppress the combinatorial background. The D_s is a spin-0 meson and the final states of both decay modes consist of a spin-1 (ϕ or K^{*0}) meson and a spin-0 (π^- or K^-) meson. The D_s signal is expected to have no dependence on $\cos\theta_p$, where θ_p is the angle in the rest frame of the D_s between the spin-0 meson direction and the D_s direction in the lab frame. However, the $\cos\theta_p$ distribution of random combinations peaks in the forward and backward directions. It is therefore required that $|\cos\theta_p| < 0.8$ (0.9) for the K^*K ($\phi\pi$) mode. The angular distribution of θ_v, the angle in the rest frame of the spin-1 meson between the direction of the final state kaon from the decay of the spin-1 meson and the D_s direction, is proportional to $\cos^2\theta_v$ for D_s decays. The $\cos\theta_v$ distribution of the random $KK\pi$ combinations in the data is, however, approximately flat. Therefore it is required that $|\cos\theta_v| > 0.4$.

3.2 $D_s^- \ell^+$ selection and decay length determination

Once a $KK\pi$ combination that satisfies the D_s candidate selection is found, a search is performed to find a lepton of opposite charge in the same jet. Electron candidates are identified using an artificial neural network based on 12 measured quantities from the electromagnetic calorimeter and the central tracking detector [10]. Electron candidates identified as arising from photon conversions are rejected [11]. Muons are identified by associating central detector tracks with track segments in the muon detectors and requiring a position match in two orthogonal coordinates [11]. Lepton candidates are required to have a momentum greater than 2 GeV/c for electrons and 3 GeV/c for muons. The leptons must have a transverse momentum with respect to the associated jet direction of at least 0.8 GeV/c. In addition it is required that the lepton candidate track be precisely measured by either the silicon vertex detector or the vertex drift chamber.

In order to suppress background, it is required that the mass of the $KK\pi\ell$ combination be between 3.2 and 5.5 GeV/c^2, and the momentum of this combination must be at least 17 GeV/c. The cosine of the opening angle between the $KK\pi$ and lepton directions must be greater than 0.4.

Three vertices — the beam spot, the B_s^0 decay vertex and the D_s decay vertex — are reconstructed in the x-y plane. The beam spot is measured using charged tracks in the OPAL data with a technique that follows any significant shifts in the beam spot position during a LEP fill [12]. The intrinsic width of the beam in the y direction is taken to be 8 μm, from considerations of LEP beam optics. The width in the x direction is measured directly and found to vary between 100 μm and 160 μm, depending on the LEP optics.

The D_s vertex is formed from a fit using the $KK\pi$ candidate tracks. The B_s^0 decay vertex is formed by extrapolating the $KK\pi$ momentum vector from its decay vertex to the intersection with the lepton track. The D_s decay length is the distance between these two decay vertices. The B_s^0 decay length is found by a fit between the beam spot and the reconstructed B_s^0 decay vertex using the direction of the $KK\pi\ell$ momentum vector as a constraint. The two-dimensional projections of the B_s^0 and D_s decay lengths are converted into three dimensions using the polar angles reconstructed using the momenta of the $KK\pi\ell$ and $KK\pi$, respectively. Typical decay lengths are about 0.25 cm for B_s^0 and 0.11 cm for D_s mesons. The corresponding typical decay length errors are about 0.03 and 0.09 cm.

Additional criteria are used to select $KK\pi$ combinations suitable for precise decay length measurements. In order to ensure that the $KK\pi$ candidate tracks come from a common vertex, the χ^2 of the vertex fit is required to be less than 10 (for 1 degree of freedom). The candidate must also have a decay length error less than 0.3 cm. Using the measured decay length and momentum of the $KK\pi$ combination, the proper decay time of the D_s candidate is determined. This is required to be within two standard deviations of the range from zero to four D_s mean lifetimes. Finally, the decay length error of the reconstructed B_s^0 candidate must be less than 0.2 cm.

3.3 Results of $D_s^- \ell^+$ selection

The $KK\pi$ invariant mass distribution for all $K^+K^-\pi^-\ell^+$ candidates is shown in figure 1. An unbinned likelihood fit to the measured $KK\pi$ invariant mass of the D_s candidates is performed. The $KK\pi$ mass distribution is parameterized as the sum of a linear term to account for random combinatorial background, a Gaussian function which describes the mass peak of the reconstructed D_s signal, and another Gaussian to account for a $D^- \to K^+K^-\pi^-$ contribution. This last term has a mean fixed to the D^- mass of 1869.3 MeV/c^2 [1] and the width constrained to be the same

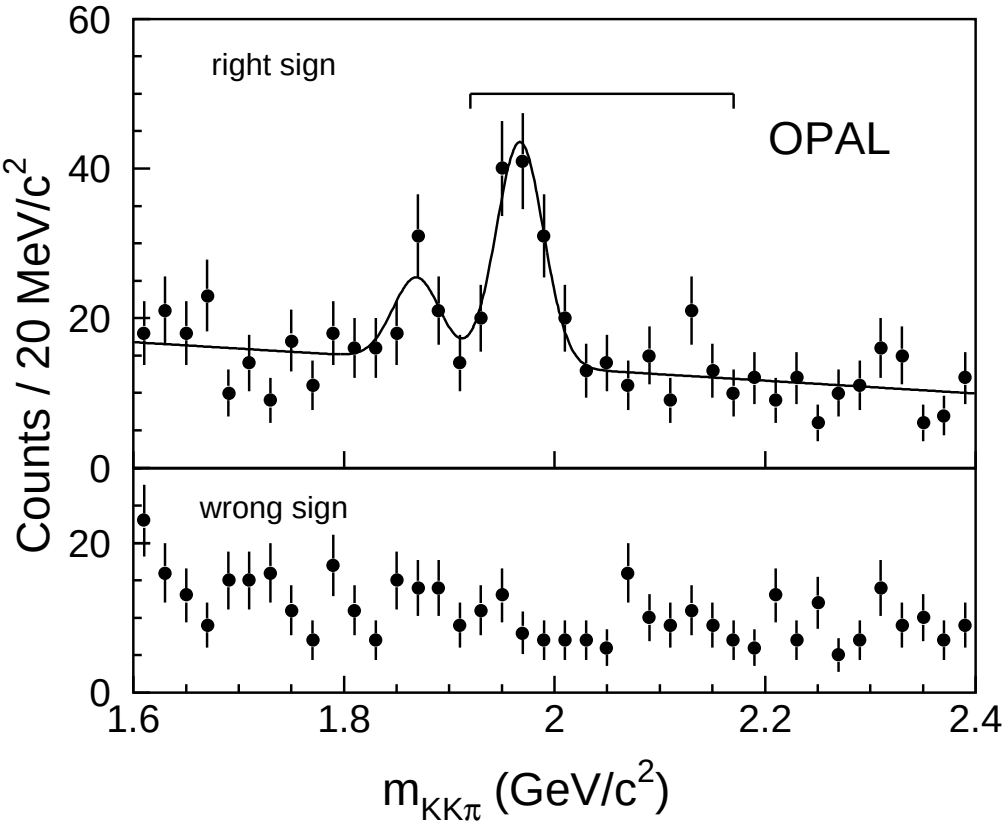

Figure 1: *Top: the* $\mathrm{KK}\pi$ *invariant mass distribution is shown for* $\mathrm{K^+K^-}\pi^-\ell^+$ *combinations along with the fitted curve, which is described in the text. Also indicated is the mass range used in the decay length fit. Bottom: the* $\mathrm{KK}\pi$ *invariant mass distribution for* $\mathrm{K^+K^-}\pi^-\ell^-$ *(wrong sign) candidates is shown.*

as that of the D_s peak. It is included in order to avoid biasing the estimate of the combinatorial background. The fit yields a D_s mass of $1.967 \pm 0.004\,\mathrm{GeV}/c^2$, a width ($\sigma$) of $22 \pm 3\,\mathrm{MeV}/c^2$ and a total of 84 ± 13 candidates. The fitted combinatorial background fraction is 0.43 ± 0.05 for the 2σ interval about the fitted D_s mass.

By integrating the tail of the peak due to the $D^- \to K^+K^-\pi^-$ decays in this D_s signal region, the contamination from this source is found to be negligible. No peak is observed at the D_s mass in the wrong sign $D_s^-\ell^-$ sample (see figure 1). The probability that a given event comes from combinatorial background is calculated as a function of its $KK\pi$ invariant mass using the results of the fit to the mass distribution for use in the B_s^0 lifetime fit discussed below.

3.4 Backgrounds to the $B_s^0 \to D_s^-\ell^+$ signal

Potential sources of backgrounds to the $B_s^0 \to D_s^-\ell^+$ signal that have been considered include decays of other B hadrons that can yield a final state $D_s\ell$ combination and charm hadrons that are mis-identified as a D_s meson. Other sources are D_s mesons combined with a hadron that has been mis-identified as a lepton, and random associations of D_s mesons with genuine leptons.

The signal events mentioned above include properly reconstructed $D_s\ell$ combinations that do not arise from B_s^0 decay. Two decay modes of B^0 and B^+ mesons have been considered: $B \to D_s^+\overline{D}(X)$, $\overline{D} \to \ell^- X$ (where $\overline{D}$ is any non-strange charm meson) and $B \to D_s^- K\ell^+\nu(X)$, where K is any type of kaon. For the signal mode, the production branching fraction $f(\overline{b} \to B_s^0) \cdot \mathrm{Br}(B_s^0 \to D_s\ell) = 2.8 \pm 0.7\%$ is used [13]. Monte Carlo simulations of both a standard multihadronic sample and the specific decay modes of interest are used to determine the selection efficiencies for these modes relative to that of the signal mode. These samples were produced using the JETSET 7.3 parton shower Monte Carlo generator [14] with the fragmentation function of Peterson *et al.* [15] for heavy quarks, and then passed through the full OPAL detector simulation package [16].

For the background, the probability for a bottom quark to form a B^+ or B^0 meson is 0.81 ± 0.11 [17]. For the $B \to D_s^- K\ell^+\nu X$ mode, a theoretical estimate [18] that predicts an upper limit of $0.025 \cdot \mathrm{Br}(B \to D\ell\nu)$ is used. This is slightly stronger than the present measured upper limit [1]. For the other background mode, it is noted that $\mathrm{Br}(B \to D_s X) = 0.085 \pm 0.011$ [1] and assumed that all of the modes of $B \to D_s X$, aside from the assumed $B \to D_s K\ell\nu X$ contribution, are of the form $B \to D_s\overline{D}X$. This has been shown to be the case for two-body decays of the B mesons to a D_s [1], and we assume the same for those modes with three or more particles in the final state. The fraction of $B \to D_s X$ decays that are in a two-body final state is 0.57 ± 0.10 [19]. Thus the fraction of $B \to D_s\bar{D}X$ decays that are expected to be a two-body final state is determined by correcting for the assumed presence of the $B \to D_s K\ell\nu X$ mode. It is assumed that the average branching fraction of the $\overline{D}$ meson to e and μ combined is 0.20 ± 0.05, and the fraction of these $\overline{D}$ mesons which come from orbitally excited states is estimated to be $0.3^{+0.7}_{-0.3}$. Thus, with an observed signal of 84 $D_s^-\ell^+$ pairs, 1.9 ± 1.8 candidates from $B \to D_s^- K\ell^+\nu X$ decays, and 2.8 ± 2.6 events in the mode $B \to D_s^+\overline{D}X$, $\overline{D} \to \ell^- X$ are expected.

The background from events where the three $KK\pi$ candidate tracks come either from the same fully reconstructed charm hadron for which a pion or a proton has been mis-identified as a kaon, or from a partially reconstructed charm hadron, was estimated using simulated events. For these candidates the $KK\pi$ invariant mass distribution around the D_s mass is similar to that of the combinatorial background. Such events are therefore considered to be included in the combinatorial background fraction.

The background caused by a D_s which has been combined with a hadron that has been misidentified as a lepton can be estimated by fitting the $KK\pi$ mass spectrum of wrong sign combinations ($K^+K^-\pi^-\ell^-$). This assumes that random combinations are equally likely to have right and wrong charge correlations. Using the higher statistics available when $D^*\ell$ correlations are considered it is found that this background is less than 1% [10] of that sample and this contribution is therefore neglected. Similarly, no signal is observed when this is repeated with the $D_s^-\ell^-$ candidates of this analysis.

Finally the background from random associations of D_s mesons with genuine leptons was estimated using simulated data to contribute less than one event to our sample and has been neglected.

Thus the non-combinatorial background for the sources mentioned above is expected to contain 4.7 ± 3.1 events, corresponding to $(6 \pm 5)\%$ of the total $D_s\ell$ signal. The number of signal candidates from $B_s^0 \to D_s^-\ell^+X$ decays which proceed through the chosen decay chains is then

$$N(B_s^0 \to D_s^-\ell^+X) \;=\; 79 \pm 13 \; .$$

4 The B_s^0 Lifetime Fit

In order to extract the B_s^0 lifetime from the measured decay lengths, an unbinned maximum likelihood fit is performed using a likelihood function that accounts for both the signal and background components of the sample. For the component of the likelihood function describing the B_s^0 signal, the B_s^0 lifetime must be related to the observed decay lengths.

Since at least the energy of the neutrino is missing, the B_s^0 energy is estimated using a probabilistic approach described in more detail in reference [20]. This method employs two kinematic variables related to the B_s^0 energy: the invariant mass and energy of the $D_s\ell$ combination. From the decay kinematics assuming the neutrino to be the only particle missing from the decay, it is possible to calculate the B_s^0 energy, given these two observables and the angle between the $D_s\ell$ flight direction in the B_s^0 rest frame and the momentum of the B_s^0 in the lab frame. Although this angle is not measured its distribution is known due to the isotropic nature of the decay of spin-0 mesons, such as the B_s^0. This, together with an estimate of the B_s^0 fragmentation spectrum is used to predict the range and distribution of the possible B_s^0 energies on an event-by-event basis. A Peterson function [15] is used for this fragmentation spectrum, though the resulting energy estimate depends only weakly on this assumption. The presence of particles, in addition to the neutrino, which come from the B_s^0 decay but are not included in the B_s^0 reconstruction, such as a photon when the B_s^0 has decayed into a D_s^* or an additional pion, is expected to bias the mean boost by less than 1%.[3]

The likelihood function for observing a particular decay length of a B_s^0 meson may now be parameterized in terms of the measurement error of the decay length, the $D_s\ell$ invariant mass and momentum, and the assumed lifetime. Specifically, this function is given by the convolution of three terms: an exponential whose mean is the B_s^0 lifetime, the boost distribution as given by the values of the observed $D_s\ell$ mass and momentum, and a Gaussian resolution function whose width is the measured decay length error.

As previously discussed, the dominant sources of *non*-combinatorial backgrounds to the process $B_s^0 \to D_s\ell$ are all cases in which the D_s and lepton both result from B^+ or B^0 decay, either

[3]The production of orbitally excited strange D mesons will not contribute to our sample as these are expected to decay to a DK pair, and not a D_s.

directly or in a subsequent decay. The likelihood function to describe these sources of background is therefore taken to have the same form as the B_s^0 signal, except that the lifetime for this sample is fixed to 1.6 ps, which is consistent with the measured average B hadron lifetime [21] and the lifetimes of the B^+ and B^0 hadrons [20]. The level of this background is a fixed fraction of the signal, as determined in the previous section. The effects of the uncertainty in this fraction on the lifetime are addressed as a systematic error.

The fit must also account for the combinatorial background present in the $D_s\ell$ sample. The functional form used to parameterize this source of background is composed of a positive and a negative exponential, each convolved with the same boost function and Gaussian resolution function as is the signal. The parameters describing these exponentials, and the fraction of each, are free parameters in the fit. This double-exponential shape is motivated by considerations of event topologies that can lead to negative apparent decay lengths, even before resolution effects are considered.

The background present in the event sample is taken into account by simultaneously fitting for the signal B_s^0 decays and background contributions. The expected combinatorial background probability is determined for each candidate using the results of the fit to the $KK\pi$ invariant mass spectrum. For the lifetime fit, the 253 events found in the region from $50\,\mathrm{MeV}/c^2$ below the fitted D_s mass to $200\,\mathrm{MeV}/c^2$ above it are used (see figure 1). This avoids the region where the number of $KK\pi$ candidates from D^- decays is significant.

The result of the fit to the decay lengths of the 253 candidates that are within the selected $KK\pi$ invariant mass region gives $\tau(B_s^0) = 1.55^{+0.25}_{-0.21}\,\mathrm{ps}$, where the error is statistical only. The decay length distributions are shown in figure 2 for those candidates with $KK\pi$ invariant mass within $50\,\mathrm{MeV}/c^2$ of the fitted D_s mass, and for those above this region. These illustrate the quality of the fit in regions dominated by signal events and by combinatorial background, respectively. The curves in figure 2 represent the sum of the decay length probability distributions for each event. The figures indicate that the fitted functional forms provide a good description of the data for both signal and background. It should be noted that the fit is to the unbinned data.

5 Evaluation of Systematic Errors

The sources of systematic error considered are those due to the level, parameterization and source of the background, the potential bias from the selection and fitting procedure, the boost estimation method, the beam spot determination and possible tracking errors.

To determine the effect of the uncertainty in the level of combinatorial background in the $D_s^-\ell^+$ candidates, both the uncertainty in the level of background as determined by the fit to the $KK\pi$ mass spectrum and the statistical variation of the background under the D_s peak have been considered. This is done by repeating the fit to the $KK\pi$ invariant mass spectrum with the background fraction constrained to be 37% and 49% and using the resulting event-by-event background probabilities in the lifetime fit. This yields a variation in the B_s^0 lifetime of $\pm 0.03\,\mathrm{ps}$. The width of the sideband region of the $KK\pi$ mass spectrum, from which candidates are selected for use in the lifetime fit, has also been varied, resulting in a change in the fitted lifetime value of $\pm 0.01\,\mathrm{ps}$. Several alternative parameterizations have been investigated. For example, terms to allow for a small subset of the candidates in which tracks have been significantly mis-measured and combinatorial background with zero lifetime have been used. In all cases, these additional terms do not significantly improve the quality of the fit. The approach used in our previous publication [4] of having a signal region with a fixed background and a sideband region assumed to have no signal, has also been applied.

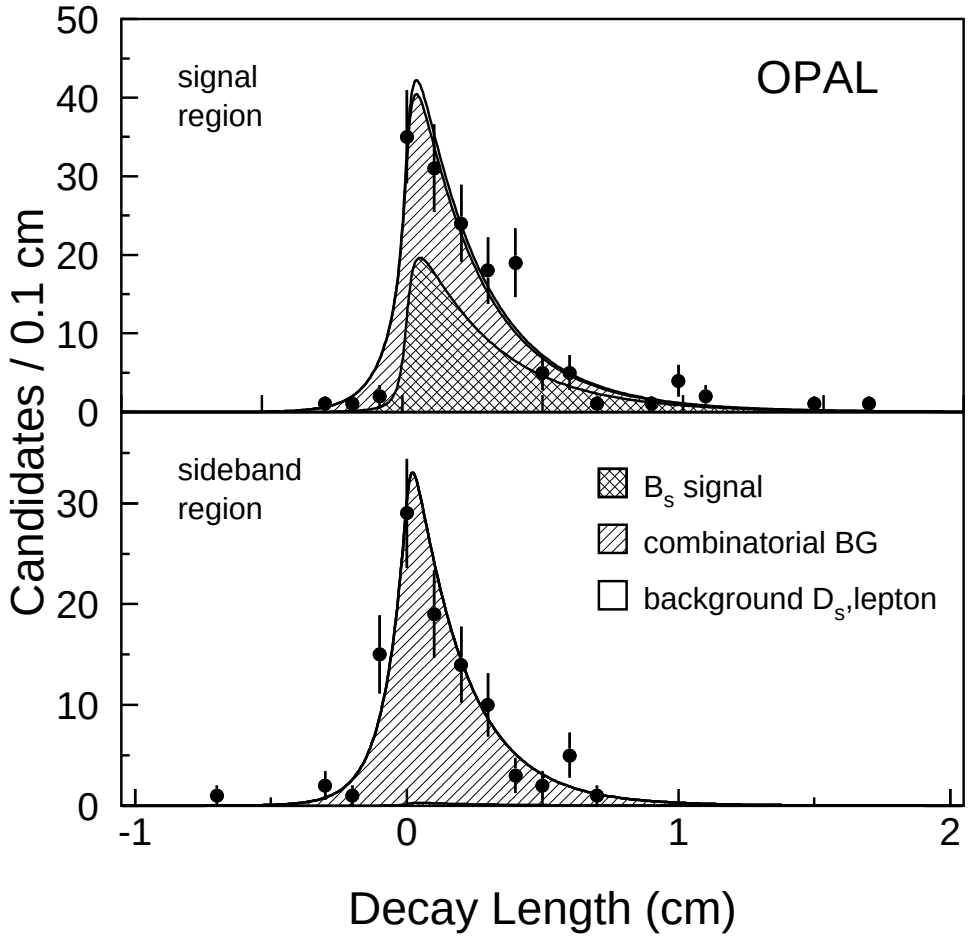

Figure 2: *Top: The decay length distribution of* $\mathrm{K^+K^-\pi^-\ell^+}$ *combinations with* $\mathrm{KK\pi}$ *mass within the* $\mathrm{D_s}$ *mass region, defined as* $\pm 50\,\mathrm{MeV}/c^2$ *around the fitted* $\mathrm{D_s}$ *mass. The single-hatched area represents the contribution from combinatorial background and the unhatched area is due to background from decays with a true* $\mathrm{D_s}$ *and lepton. Bottom: The decay length distribution of* $\mathrm{K^+K^-\pi^-\ell^+}$ *combinations with* $\mathrm{KK\pi}$ *mass outside the* $\mathrm{D_s}$ *mass region. These candidates have* $\mathrm{KK\pi}$ *mass in the range from* $50\,\mathrm{MeV}/c^2$ *to* $200\,\mathrm{MeV}/c^2$ *above the fitted* $\mathrm{D_s}$ *mass. The curves are described in the text.*

The difference in the fitted lifetime when this approach is used is less than $+0.01$ ps. The effect of the backgrounds involving $D_s\ell$ that are not from the decay of a B_s^0 meson, namely from either B^+ or B^0 decays, was also considered. The level of this non-combinatorial background was found to be $(6 \pm 5)\%$. The variation in the level of this background over the given range corresponds to an uncertainty of ± 0.01 ps. The lifetime of this background is fixed to 1.6 ps for the nominal result and is varied by ± 0.10 ps to account for the uncertainty in this value. This variation results in changes to the B_s^0 lifetime of ± 0.01 ps. Thus we assign a total error due to the background fraction, parameterization and source of ± 0.03 ps.

Tests were performed on several samples of simulated data to check for biases in the selection and fitting methods. The results of these tests are consistent with there being no bias: the ratio of the fitted lifetime to the generated lifetime is 1.01 ± 0.02. Nonetheless, we correct our determination of the B_s^0 lifetime by this factor and take the statistical precision of this ratio as a potential selection and fitting bias by assigning a systematic error of ± 0.03 ps.

The estimated B_s^0 energy spectrum that is used by the boost estimation procedure has been varied within the measured limits of the average b hadron energy [22] to yield a variation in the B_s^0 lifetime of ± 0.02 ps. The effect of a 6 MeV/c^2 uncertainty in the mass of the B_s^0 [23] was found to produce a change of less than 0.01 ps in the B_s^0 lifetime. A number of alternative methods of boost estimation were used to confirm the method used for the principle result. A method whereby a mean boost is analytically calculated for each event (as used in the previous B_s^0 lifetime publication[4]) was also used and the resulting difference of $+0.01$ ps included as a systematic effect. A boost method based on the use of simulated data to estimate the boost was also used and yielded a lifetime less than 0.01 ps from the nominal result. The uncertainty in the measurement of the mass and momentum of the $D_s\ell$ combination that are used to obtain the estimate of the B_s^0 energy is found to contribute ± 0.01 ps to the error. Finally, the presence of missing particles, such as the photon when the B_s^0 has decayed into a D_s^*, changes the fitted lifetime by < 0.01 ps. An error of ± 0.01 ps is ascribed to the lifetime due to this source. The total systematic error resulting from the uncertainty in the boost estimation procedure is ± 0.03 ps.

The average intersection point of the LEP beams in OPAL is used as the estimate of the production vertex of the B_s^0 candidates. The mean coordinates of the beam spot are known to better than 25 μm in the x direction and 10 μm in y. The effective r.m.s. spread of the beam is known to a precision of less than 10 μm in both directions. To test the sensitivity of $\tau(B_s^0)$ to the assumed position and size of the beam spot, the coordinates of the beam spot are shifted by ± 25 μm, and the spreads changed by ± 10 μm. The largest observed variation in $\tau(B_s^0)$ is 0.01 ps, which is assigned as a systematic error.

The effects of alignment and calibration uncertainties on the result are not studied directly but are estimated from a detailed study of 3-prong τ decays [12], where the uncertainty in the decay length due to these effects is found to be less than 1.8% for the data taken during 1990 and 1991 and less than 0.4% for later data. This corresponds to an uncertainty on $\tau(B_s^0)$ of 0.01 ps. The potential for mis-estimation of the decay length error has been addressed by allowing an additional parameter in the lifetime fit which is a scale factor on the measured decay length error. It is found that this parameter is consistent with unity and produces a change in the B_s^0 lifetime of less than 0.01 ps.

After applying the correction due to the potential of a bias in the result, and combining the systematic errors in quadrature, we find $\tau(B_s^0) = 1.54^{+0.25}_{-0.21}(\text{stat}) \pm 0.06(\text{syst})$ ps. These systematic errors are summarized in Table 1.

Source	bias (ps)	uncertainty (ps)
background		± 0.03
possible bias of method	-0.01	± 0.03
uncertainty in boost		± 0.03
beam spot		± 0.01
alignment errors		± 0.01
total	-0.01	± 0.06

Table 1: *Summary of systematic errors on the* B_s^0 *lifetime.*

6 Conclusion

A sample of $B_s^0 \to D_s^- \ell^+ \nu(X)$ decays has been reconstructed in which the D_s^- has decayed into $K^+K^-\pi^-$ through either the $\phi\pi^-$ or $K^{*0}K^-$ channels. From 3.6 million hadronic Z^0 events recorded by OPAL from 1990 to 1994, a total of 79 ± 13 such candidates are attributed to B_s^0 decays. The B_s^0 lifetime is found to be

$$\tau(B_s^0) = 1.54^{+0.25}_{-0.21}(\text{stat}) \pm 0.06(\text{syst})\,\text{ps},$$

where the total fractional error corresponds to about 15%. As predicted by theoretical calculations [3], this result is consistent with the observed value for the B^0 lifetime [20].

Acknowledgements

It is a pleasure to thank the SL Division for the efficient operation of the LEP accelerator, the precise information on the absolute energy, and their continuing close cooperation with our experimental group. In addition to the support staff at our own institutions we are pleased to acknowledge the
Department of Energy, USA,
National Science Foundation, USA,
Particle Physics and Astronomy Research Council, UK,
Natural Sciences and Engineering Research Council, Canada,
Fussefeld Foundation,
Israel Ministry of Science,
Israel Science Foundation, administered by the Israel Academy of Science and Humanities,
Minerva Gesellschaft,
Japanese Ministry of Education, Science and Culture (the Monbusho) and a grant under the Monbusho International Science Research Program,
German Israeli Bi-national Science Foundation (GIF),
Direction des Sciences de la Matière du Commissariat à l'Energie Atomique, France,
Bundesministerium für Forschung und Technologie, Germany,
National Research Council of Canada,
A.P. Sloan Foundation and Junta Nacional de Investigação Científica e Tecnológica, Portugal.

References

[1] Particle Data Group, *Review of Particle Properties*, Phys. Rev. **D 50** (1994) 1173.

[2] G. Altarelli and S. Petrarca, Phys. Lett. **B 261** (1991) 303;
I.I. Bigi, Phys. Lett. **B 169** (1986) 101;
J.H. Kühn *et al.*, *Heavy Flavours at LEP*, MPI–PAE/PTh 49/89, August 1989, contribution by R. Rückl, p. 59.

[3] I. Bigi *et al.*, *Non-leptonic Decays of Beauty Hadrons – from Phenomenology to Theory*, (CERN-TH.7132/94), from the second edition of the book 'B Decays,' S. Stone (ed.), World Scientific, pp. 132-157;
I.I. Bigi and N.G. Uraltsev, Phys. Lett. **B 280** (1992) 271.

[4] OPAL Collab., P.D. Acton *et al.*, Phys. Lett. **B 312** (1993) 501.

[5] ALEPH Collab., D. Buskulic *et al.*, Phys. Lett. **B 322** (1994) 275;
DELPHI Collab., P. Abreu *et al.*, Z. Phys. C 61 (1994) 407;
CDF Collab., F. Abe *et al.*, *Measurement of the* B_s *Meson Lifetime*, FERMILAB-PUB-94-420-E, January 1995, to be submitted to Phys. Rev. Lett.

[6] OPAL Collab., K. Ahmet *et al.*, Nucl. Inst. and Meth. **A 305** (1991) 275;
P.P. Allport *et al.*, Nucl. Inst. and Meth. **A 324** (1993) 34;
P.P. Allport *et al.*, Nucl. Inst. and Meth. **A 346** (1994) 479.

[7] O. Biebel *et al.*, Nucl. Inst. and Meth. **A 323** (1992) 169;
M. Hauschild *et al.*, Nucl. Inst. and Meth. **A 314** (1992) 74.

[8] OPAL Collab., G. Alexander *et al.*, Z. Phys. **C 52** (1991) 175.

[9] JADE Collaboration, W. Bartel *et al.*, Z. Phys. **C 33** (1986) 23;
JADE collaboration, S. Bethke *et al.*, Phys. Lett. **B 213** (1988) 235.

[10] OPAL Collab., R. Akers *et al.*, Phys. Lett. **B 327** (1994) 411.

[11] OPAL Collab., P.D. Acton *et al.*, Z. Phys. **C 58** (1993) 523.

[12] OPAL Collab., P.D. Acton *et al.*, Z. Phys. **C 59** (1993) 183;
OPAL Collab., R. Akers *et al.*, Phys. Lett. **B 338** (1994) 497.

[13] The value quoted for $f(\bar{b} \to B_s^0) \cdot \mathrm{Br}(B_s^0 \to D_s \ell)$ is the sum of the muon and electron channels. It is an average of the following measurements:
DELPHI Collab., P. Abreu *et al.*, Phys. Lett. **B 289** (1992) 199;
ALEPH Collab., D. Buskulic *et al.*, Phys. Lett. **B 294** (1992) 145;
OPAL Collab., P.D. Acton *et al.*, Phys. Lett. **B 295** (1992) 357.

[14] T. Sjöstrand, JETSET 7.3 Manual, CERN-TH 6488/92;
The OPAL parameter set is given in
OPAL Collab., P.D.Acton *et al.*, Z. Phys. **C 58** (1993) 387.

[15] C. Peterson *et al.*, Phys. Rev. **D 27** (1983) 105.

[16] J. Allison *et al.*, Nucl. Inst. and Meth. **A 317** (1992) 47.

[17] OPAL Collab., R. Akers *et al.*, *A Study of Charm Meson Production in Semileptonic B Decays*, CERN-PPE/95-2, 11 January 95, submitted to Z. Phys. C.

[18] E. Golowich *et al.*, Z. Phys. **C 48** (1990), 89.

[19] ARGUS Collab., H. Albrecht *et al.*, Z. Phys. **C 54** (1992) 1;
CLEO Collab., D. Bortoletto *et al.*, Phys. Rev. **D 45** (1992) 21;
CLEO Collab., D. Bortoletto *et al.*, Phys. Rev. Lett. **64** (1990) 2117.

[20] OPAL Collab., R. Akers *et al.*, *Improved Measurements of the* B^0 *and* B^+ *Meson Lifetimes*, CERN-PPE/95-19, 22 February 1995, submitted to Z. Phys. C.

[21] OPAL Collab., P.D. Acton *et al.*, Z. Phys. **C 60** (1993) 217.

[22] OPAL Collab., R. Akers *et al.*, Z. Phys. **C 60** (1993) 199.

[23] ALEPH Collab., D. Buskulic *et al.*, Phys. Lett. **B 311** (1993) 425; Erratum, Phys. Lett. **B 316** (1993) 631;
CDF Collab., F. Abe *et al.*, Phys. Rev. Lett. **71** (1993) 1685;
DELPHI Collab., P. Abreu *et al.*, Phys. Lett. **B 324** (1994) 500;
OPAL Collab., R. Akers *et al.*, Phys. Lett. **B 337** (1994) 196.